

Surface acoustic wave acceleration sensor with high sensitivity incorporating ST-X quartz cantilever beam

This content has been downloaded from IOPscience. Please scroll down to see the full text.

2015 Smart Mater. Struct. 24 015015

(<http://iopscience.iop.org/0964-1726/24/1/015015>)

View [the table of contents for this issue](#), or go to the [journal homepage](#) for more

Download details:

IP Address: 124.16.131.65

This content was downloaded on 03/04/2015 at 07:27

Please note that [terms and conditions apply](#).

Surface acoustic wave acceleration sensor with high sensitivity incorporating ST-X quartz cantilever beam

Wen Wang, Yangqing Huang, Xinlu Liu and Yong Liang

State key Laboratory of Acoustics, Institute of Acoustics, Chinese Academy of Sciences, Beijing, 100190, People's Republic of China

E-mail: wangwenwq@mail.ioa.ac.cn

Received 29 July 2014, revised 24 September 2014

Accepted for publication 13 November 2014

Published 8 December 2014



CrossMark

Abstract

The implementation and performance of a surface acoustic wave (SAW)-based acceleration sensor is described. The sensor was composed of a flexible ST-X quartz cantilever beam with a relatively substantial proof mass at the undamped end, a pattern of a two-port SAW resonator deposited directly on the surface of the beam adjacent to the clamped end for maximum strain sensitivity and a SAW resonator affixed on the metal package base for temperature compensation. The acceleration was directed to the proof mass flex of the cantilever, inducing relative changes in the acoustic propagation characteristics of the SAW traveling along the beams. The frequency signal from the differential oscillation structure utilizing the SAW resonators as the feedback element varies as a function of acceleration. The sensor response mechanism was analyzed theoretically, with the aim of determining the optimized dimension of the cantilever beam. The coupling of modes (COM) model was used to simulate the synchronous SAW resonator prior to fabrication. The oscillator frequency stability was improved using the phase modulation approach; the obtained typical short-term frequency stability ranged up to 1 Hz s^{-1} . The performance of the developed acceleration sensor was evaluated using the precise vibration table and was also evaluated in comparison to the theoretical calculation. A high frequency sensitivity of 29.7 kHz g^{-1} , good linearity and a lower detection limit ($\sim 1 \times 10^{-4} \text{ g}$) were achieved in the measured results.

Keywords: surface acoustic wave, acceleration sensor, cantilever beam, oscillator, ST-X quartz, two-port resonator

(Some figures may appear in colour only in the online journal)

1. Introduction

As the core component in the inertial measurement system, the acceleration sensor is used to measure the motion status of the object utilizing its inertial properties. The acceleration sensor has seen diverse applications ranging from aviation, aerospace and astronomy to petrochemical and transportation.

Among a wide variety of acceleration sensors, the surface acoustic wave (SAW)-based acceleration sensor has gained increasing attraction for its inertial application because it exhibits some unique properties as a simple structure that is convenient to manufacturer with no auxiliary equipment; it is also low cost, has good impact resistance, offers a stable and reliable performance and has high sensitivity [1]. A typical SAW acceleration sensor employs modem resonating beam force sensing technology, which is widely used in the high precision accelerometer design [2]. The SAW devices use a piezoelectric substrate mounted as a cantilever beam to sense vibrations and convert sensed vibrations to electrical signals.



Content from this work may be used under the terms of the Creative Commons Attribution 3.0 licence. Any further distribution of this work must maintain attribution to the author(s) and the title of the work, journal citation and DOI.

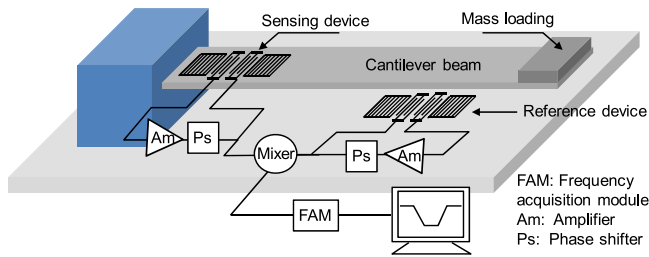


Figure 1. The schematic of the SAW acceleration sensor incorporating the cantilever beam.

The cantilever is clamped at one end, and a relatively substantial proof mass is affixed at the undamped end. Acceleration or other physically applied forces directed to the proof mass at the undamped end flex the cantilever, leading to relative changes in the acoustical propagation characteristics of the SAW traveling on the surface of the cantilever beam. The measurement of the frequency of a SAW device yields a measure of strain of the cantilever resulting from forces applied to the proof mass. Several groups have reported a SAW acceleration sensor that encompasses a variety of structures and principles. Hartemann *et al* present the first SAW accelerometer prototype using two circular quartz membranes that an inertial mass loads in flexure. A differential frequency signal from the dual-delay line oscillator was used to characterize the applied acceleration [3]. A heartening frequency sensitivity of 10 kHz g^{-1} over a 20 g acceleration range was achieved. Bower *et al* developed a SAW accelerometer using a differential structure of a dual-resonator-oscillator on a quartz beam mounted as a cantilever [4]. The achieved sensitivity and linearity in the full-scale range of 30 g were 2 kHz g^{-1} and $20 \mu\text{g g}^{-2}$, respectively. A similar structure with improved performance on the SAW accelerometer is also described by some groups after more than a decade of effort [5–8, 12]. However, as mentioned in [1], the obtained resolution threshold and the linearity error are rather poor regarding those specified in inertial guiding and navigation system accelerometers. To improve these characteristics effectively, the optimization on the mechanical design and mounting is an urgent problem to be solved. However, to our knowledge, there are few systematic theoretical studies concerning the response mechanism of the SAW acceleration sensor. Jiang *et al* provided some meaningful simulations on the design consideration of the SAW accelerometer using a ST-X quartz cantilever utilizing the ANSYS finite element [1], but it is not supported by the experimental results. Recently, the cantilever beam structure incorporating a SAW delay line pattern and the attached proof mass were also advised for small vibration detection [9–10]; some theoretical analysis is also performed on the dimension consideration of the pre-stressed cantilever beam. This provides a good starting point for the optimal design on the SAW accelerometer with a cantilever beam,

In this paper, a SAW acceleration sensor incorporating a ST-X quartz cantilever beam was developed, which utilizes a differential resonator-oscillator structure, as shown in figure 1. The sensor was composed of a flexible ST-X quartz

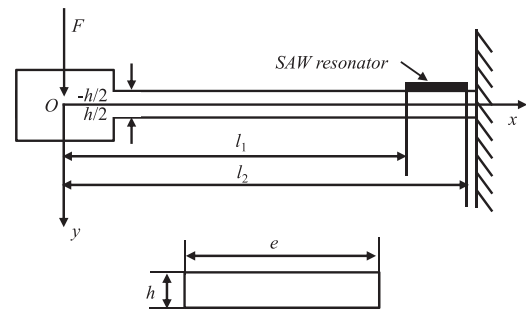


Figure 2. The static model of the acceleration sensor with the cantilever beam.

cantilever beam with a relatively substantial proof mass at the undamped end, a pattern of a two-port SAW resonator with an operating frequency of 300 MHz deposited directly on the surface of the beam adjacent to the clamped end for maximum strain sensitivity and a SAW resonator affixed on the metal package base for temperature compensation. ST-X quartz was chosen as the material for the cantilever owing to its satisfactory temperature stability and good strain sensitivity [11], and it provides a SAW velocity of 3158 m s^{-1} and electro-mechanical coupling constants of 0.12% . The two resonators were used as the control element of an oscillator; the outputs of the two oscillators are mixed, and the difference frequency signal of the mixer is amplified, picked up by the frequency acquisition module (FAM) and recorded by the PC. The acceleration was directed to the proof mass flex of the cantilever, inducing relative changes in the acoustic propagation characteristics of the SAW traveling along the beams. The measurement of the oscillation frequency shift yields a measure of applied acceleration.

Using the Rayleigh method [9–12], the response mechanism of the acceleration sensor was established theoretically, which allows us to obtain analytical expressions of the acceleration sensitivity. The effects on the sensor response from the geometric structure of the cantilever were analyzed in detail. Hence, the optimal design on the dimensions of the cantilever beam and affixed proof mass were determined. To improve the detection limit, a single resonance design utilizing the COM model and phase modulation approach was used for the resonator-oscillator to improve the oscillator frequency stability [13]. The performance of the developed SAW acceleration sensor toward the applied acceleration was evaluated by the programmable precise vibration table. Good frequency sensitivity, a lower detection limit and excellent linearity were achieved experimentally.

2. Theoretical background

2.1. Sensor response mechanism

For the theoretical approach of the response mechanism of the SAW-acceleration-sensor-incorporating cantilever beam, a structure composed of a ST-X quartz cantilever beam with a rectangular section, SAW devices located on the beam surface

and a proof mass affixed on the undamped end were constructed, as shown in figure 2. The length, width and thickness of the cantilever beam are indicated as l , e and h , respectively. Also, to simplify the numerical solution, the ST-X quartz beam is assumed as an isotropic medium. The inertial force F ($F=ma$, m and a are the proof mass and applied acceleration, respectively) is from the applied acceleration directed to the proof mass and induces shifts in stress σ_{Ax} and the strain (longitudinal and transverse: ε_x and ε_y) along the beam, which are expressed as

$$\sigma_{Ax} = \frac{Fx(-h/2)}{J} = -\frac{Fhx}{2J}, \quad (1)$$

and

$$\varepsilon_x = \frac{F}{EJ} \cdot \frac{h}{2}x, \quad \varepsilon_y = -\mu \frac{F}{EJ} \cdot \frac{h}{2}x$$

$$J = \frac{eh^3}{12} \quad (2)$$

Here, μ and E are the Poisson's ratio and elastic modulus of the quartz cantilever. J is the rotational inertia. So, the average strain distribution in the effective resonance cavity of the SAW resonator on the clamped end of the cantilever is given by

$$\bar{\varepsilon}_x = \int_{l_2}^{l_1} \left(\frac{F}{EJ} \cdot \frac{h}{2}x \right) dx = \frac{F}{EJ} \cdot \frac{h}{2}(l_2 + l_1).$$

$$\bar{\varepsilon}_y = -\mu \frac{F}{EJ} \cdot \frac{h}{4}(l_2 + l_1) \quad (3)$$

For the acceleration sensor, the inertial force F directed to the proof mass flexes the cantilever beam and changes the center distance of interdigital electrodes d . Also, the shift in strain along the cantilever beam will induce the changes in the density ρ and elastic modulus E and, accordingly, the shifts of the SAW velocity v_s and wavelength λ . The SAW wavelength λ changes as a function in strain, and it is given by

$$\lambda = \lambda_0(1 + \bar{\varepsilon}_1) = 2d. \quad (4)$$

The relationship between the SAW velocity and the strain is given by

$$v_s = v_{s0}(1 + r_1\bar{\varepsilon}_1 + r_2\bar{\varepsilon}_2) \quad (5)$$

Here, $\bar{\varepsilon}_1$ and $\bar{\varepsilon}_2$ are the average flexing strain parallel and perpendicular to the surface acoustic wave propagation direction, respectively. r_1 and r_2 are the strain coefficients, and v_{s0} and λ_0 are the undisturbed SAW velocity and wavelength, respectively. So, the resonance frequency shift, Δf , depending on the changes in strain induced by the inertial force, can be expressed from equations (4) and (5) as

$$f(\varepsilon) = \frac{v_s(\varepsilon)}{\lambda(\varepsilon)} = f_0 \frac{1 + r_1\bar{\varepsilon}_1 + r_2\bar{\varepsilon}_2}{1 + \bar{\varepsilon}_1}, \quad (6)$$

$$\Delta f = f - f_0 = \frac{(r_1 - 1)\bar{\varepsilon}_1 + r_2\bar{\varepsilon}_2}{1 + \bar{\varepsilon}_1} f_0, \quad (7)$$

where f_0 is the undisturbed resonance frequency. The $\bar{\varepsilon}_1$ in the

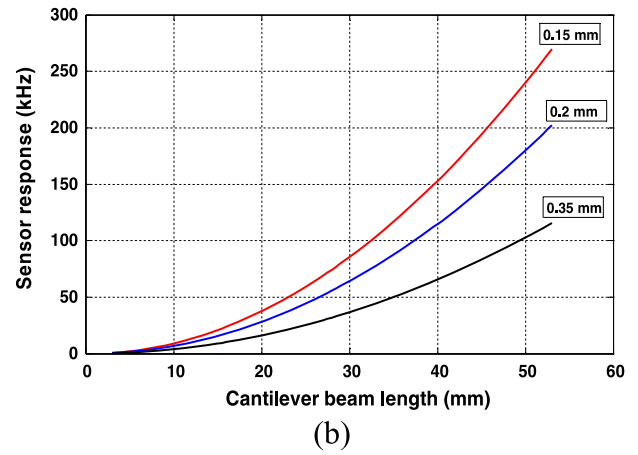
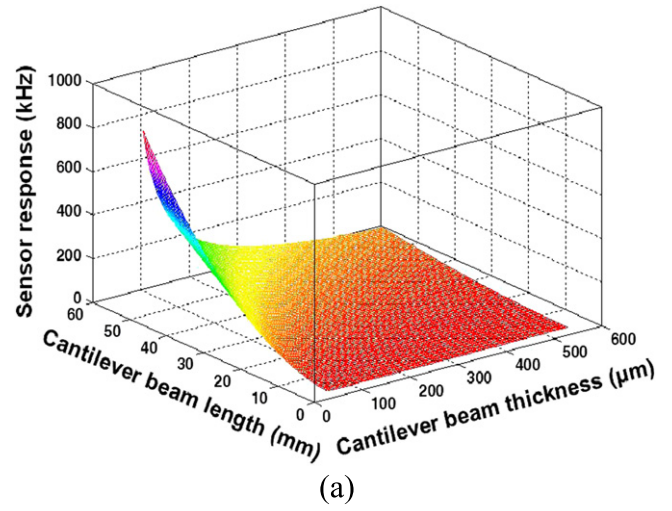


Figure 3. The calculated relationship among the sensor response and the cantilever beam length and thickness, applied acceleration: 1 g.

denominator of equation (7) can be ignored when $\varepsilon < 10^{-3}$; so, equation (7) can be rewritten as

$$\Delta f = ((r_1 - 1)\bar{\varepsilon}_1 + r_2\bar{\varepsilon}_2)f_0. \quad (8)$$

Then, substituting $\bar{\varepsilon}_1 = \bar{\varepsilon}_x$, $\bar{\varepsilon}_2 = \bar{\varepsilon}_y$ into equation (8), the relationship between the resonance frequency response and applied acceleration a can be described as

$$\Delta f = \frac{F}{EJ} \cdot \frac{h}{4}(l_2 + l_1)((r_1 - 1) - \mu r_2)f_0$$

$$= \frac{3ma}{Eeh^2}(l_2 + l_1)((r_1 - 1) - \mu r_2)f_0, \quad (9)$$

As mentioned in equation (9), the sensor frequency response relates to the geometric structure of the cantilever beam and proof mass. The larger mass loading and the longer and thinner cantilever will significantly contribute to the sensitivity of the apparatus. However, all of these rapidly reduce the natural resonance frequency of the cantilever while improving the acceleration sensitivity. It is well known that the sensor chip is easy to destroy when the resonance frequency of the cantilever is close to the dynamic load

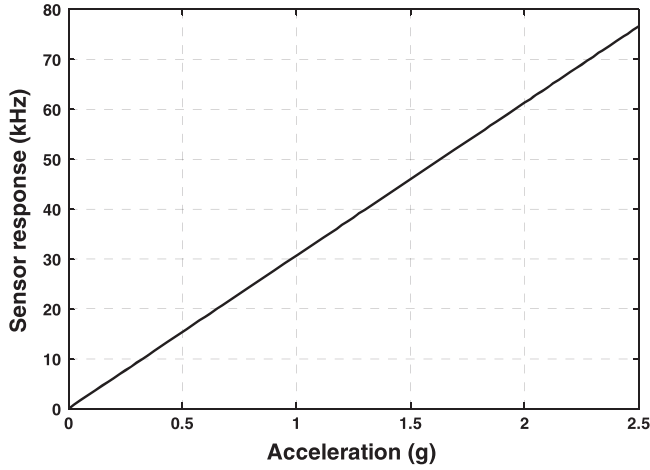


Figure 4. The calculated acceleration sensitivity and cantilever length and thickness are 20 mm and 0.2 mm, respectively.

frequency. Therefore, a higher resonance frequency of the beam is essential for the acceleration of the sensor design. Referring to the Rayleigh method and using the determined Young's modulus, the resonance frequency of the beam, f_{res} , can be given by

$$f_{res} = \frac{1}{2\pi l} \sqrt{\frac{3EJ}{\rho e h \left(\frac{33}{140} + \gamma \right)}}, \quad (10)$$

where, γ is the proof mass and the mass of the beam ratio.

2.2. Numerical results and discussion

The relationship among the sensor response toward the given acceleration of 1 g and the dimension of the cantilever beam was calculated, as shown in figure 3 using equation (9) and the simulation parameters listed in table 1. From the picture, the sensor response increases significantly using the longer and thinner beam. However, to avoid the resonance phenomena between the dynamic load and the cantilever beam, a higher resonance frequency of the beam is essential, and we can assume the frequency up to 500 Hz in this study. So, according to equation (10), for a ST-X quartz cantilever beam with a thickness of 0.2 mm, the length should be less than 20 mm when the proof mass and the beam mass ratio is set to 5. Notably, the width of the cantilever does not significantly contribute to the sensor response and resonance frequency, as mentioned in equations (9) and (10); so, the width of the beam is considered as a constant, and it is set to 1.5 mm in our study. Consequently, the dimension of the cantilever is determined as 1.5 mm × 20 mm × 0.2 mm in case the proof mass and the beam mass ratio is 5. Based on the determined design parameters, the sensitivity of the sensor can be calculated as shown in figure 4; a frequency sensitivity of ~30.4 kHz g⁻¹ is expected.

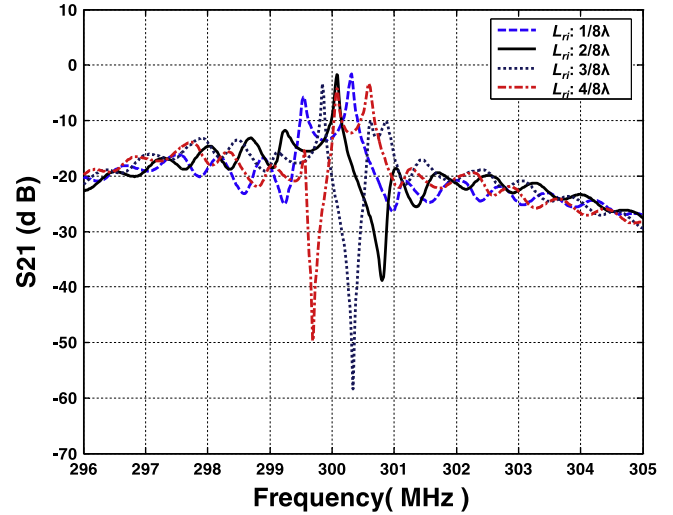


Figure 5. The calculated L_{ri} dependence of the frequency response of the resonator by using the COM model.

3. Devices and fabrication

3.1. COM simulation on the SAW resonator

Prior to the fabrication of the sensor chip, the design parameters of the SAW resonator were determined using the COM simulation. The aim is to obtain low insertion loss, single resonance and high quality value. COM modeling is a very efficient technique developed for analyzing the SAW devices [13]. For the optimal simulation on the two-port SAW resonator configuration composed of two interdigital transducers (IDTs) and the adjacent reflectors (figure 5), a COM model was used to analyze the IDTs and reflectors, respectively. By using the extracted mixed P-matrix of the IDTs, the reflectors and the gaps between the IDTs and reflectors, the device admittance matrix Y can be deduced; hence, the frequency response, S_{12} , of the SAW resonator is given by

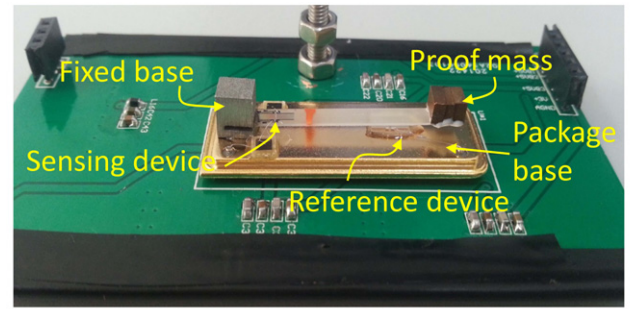
$$S_{21} = \frac{-2y_{12} \sqrt{G_{in} G_{out}}}{(G_{in} + y_{11})(G_{out} + y_{22}) - y_{12} y_{21}}, \quad (11)$$

where G_{in} and G_{out} are the input and output impedance, respectively; y_{11} , y_{12} , y_{21} and y_{22} are the admittance matrix elements. Utilizing equation (11), the frequency response of the two-port SAW resonator can be simulated. Usually, the most critical parameter for the resonator design is the spacing L_{ri} between each grating reflector and its adjacent IDT [14]. The simulation was performed in terms of different values of L_{ri} to extract the optimal design parameters. The IDTs with 41λ (λ is the wavelength at a given operation frequency) and an aperture of 100λ were chosen for this simulation. The other simulation parameters of the resonator are the ST-X quartz substrate, an operation frequency of 300 MHz, a shorted grating reflector with 300 electrodes and 10.25λ spacing between the IDTs. Figure 5 shows the L_{ri} dependence of the frequency response of the resonator. To obtain a single steep resonance peak with low insertion loss, an L_{ri} of $1/4\lambda$ was chosen in the synchronous design.

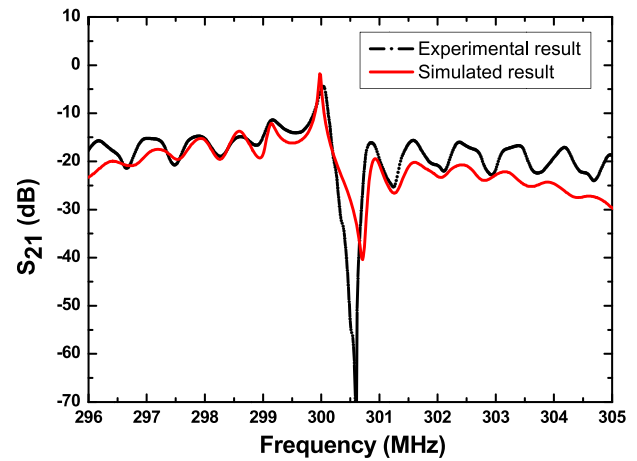
3.2. Sensor chip

Based on the extracted optimal design parameters for the SAW resonator and cantilever beam listed in table 2, the chip for the acceleration sensor was reproducibly fabricated by the standard photolithographic technique. As shown in figure 1, the sensor is composed of two resonators, one is for acceleration sensing, and the other is used for temperature compensation. The operation frequencies of the resonators are designed to operate at 300 MHz and 300.5 MHz, which provides a differential frequency of 0.5 MHz for acceleration sensing. The number of IDT finger pairs and reflector electrodes of the two resonators are both set to 41 and 300; the finger widths are $2.631 \mu\text{m}$ and $2.627 \mu\text{m}$, respectively. The spacing between the IDTs and adjacent reflectors are both set to 0.25λ . The apertures of the resonators are both designed to 80λ . The schematic diagrams of the fabrication procedure are described below: Aluminum of a $\sim 150 \text{ nm}$ thickness was first deposited onto the ST-X quartz substrate with 0.2 mm thickness using an electron beam evaporator. Then, the photoresist (PR) was spin-coated, exposed and then patterned for IDTs and the adjacent shorted grating reflectors. Next, the aluminum was wet-etched in $4\text{H}_3\text{PO}_4:1\text{HNO}_3:4\text{CH}_3\text{COOH}:1\text{H}_2\text{O}$ etchant. The PR was dissolved in acetone. Several rinses with DI water were performed to remove any unwanted products. Then, the substrate was dicing-sawed for packaging according to the determined dimension ($1.5 \text{ mm} \times 20 \text{ mm}$) and mounted as a cantilever beam using the fixed base made by Al. The proof Al mass with five times the mass of the cantilever beam is glued at the undamped end of the beam. Next, the fixed base is affixed firmly onto the metal package base, as shown in figure 6(a). Another dicing-sawed SAW resonator with a size of $1.5 \text{ mm} \times 3 \text{ mm}$ was placed on the package base as the reference for the temperature compensation. The fabricated SAW resonators were characterized using the network analyzer E5071B; the measured operation frequencies of two resonators are 299.95 MHz and 300.37 MHz, and they have little deviation from the predetermined design because of technical reasons. The typical frequency response of the sensing resonator is characterized, as shown in figure 6(b); a low insertion loss of 3.7 dB, a high unloaded Q-value of ~ 3000 and a single-mode were obtained. Also, the measured frequency response agrees well with the COM simulated results.

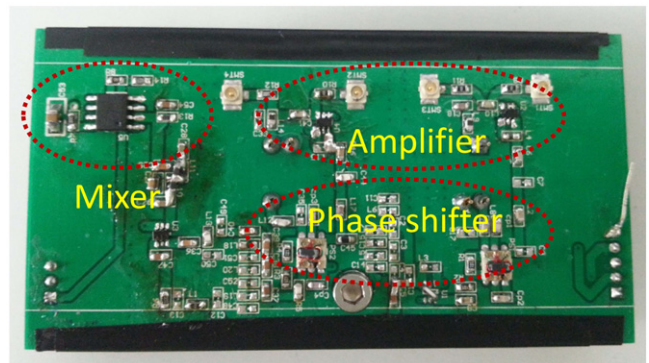
Next, the fabricated SAW resonators were used as the control element of an oscillator and were connected to each oscillation circuit, which was made of discrete elements (amplifier with a gain of 15 dB, phase shifter, mixer, LPF, and so on). Then, the outputs of each oscillator are mixed (figure 6(c)), picked by the FAM and recorded by the PC. To improve the frequency stability, the oscillation was modulated at the frequency point with the lowest insertion loss by a strategic phase modulation [11]. Typical short-term (s), medium-term (1 h) and long-term (1 d) frequency stability of the developed resonator-oscillator were characterized as 1 Hz s^{-1} , 25 Hz h^{-1} (0.08 ppm) and 50 Hz d^{-1} (0.17 ppm) at room temperature (20°C), respectively. Figure 7 shows the



(a)



(b)



(c)

Figure 6. (a) The developed SAW acceleration sensor chip, (b) the measured S_{21} of the SAW resonator and (c) the oscillation circuit.

typical medium-term frequency stability at a stable status of the developed resonator-oscillator. The mixed output of the resonator-oscillators is $\sim 415 \text{ kHz}$. The excellent frequency stability observed from the fabricated oscillator is very significant for detection limit improvement of the SAW sensor [12].

4. Experimental results and discussion

The experimental set-up used for characterizing the acoustic sensing device is composed of the developed SAW-based accelerometer system, the PC, the precision vibration table and the commercial accelerometer for calibration, as shown in

Table 1. Simulation parameter of the SAW acceleration sensor.

	r_1	r_2	$E \text{ N} \cdot \text{m}^{-2}$	μ	$\rho \text{ kg} \cdot \text{m}^{-3}$
ST-X quartz	-0.002 ± 0.044	-0.164 ± 0.01	8.3×10^{10}	0.26	2631

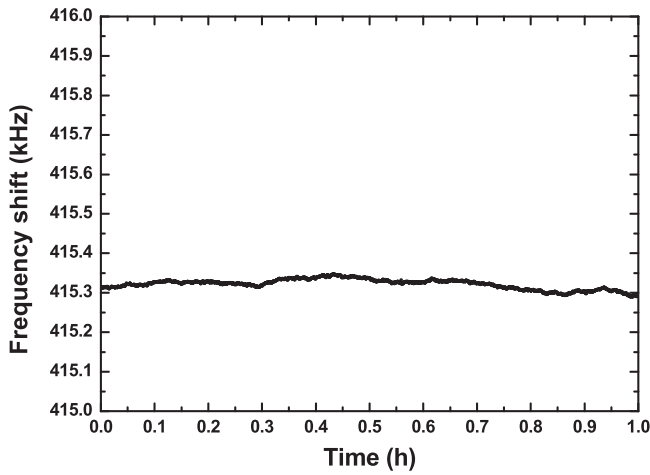


Figure 7. The measured medium-term frequency stability of the SAW oscillator.

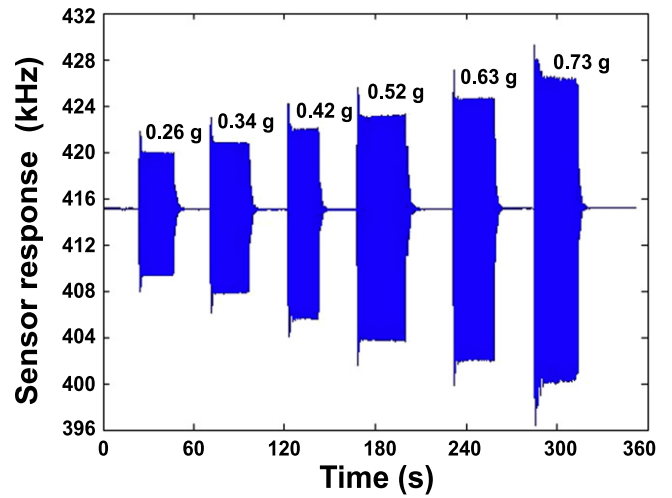


Figure 9. The transient response of the acceleration sensor, depending on the acceleration.



Figure 8. The measurement set-up of the SAW acceleration sensor.

figure 8. The SAW accelerometer system was bolted firmly to the vibrating table. A self-made interface display program was used to record the vibration status of the SAW accelerometer. The precision vibration table provides an acceleration range of 0~20 g with varying vibration frequency, and the applied acceleration is monitored using the commercial

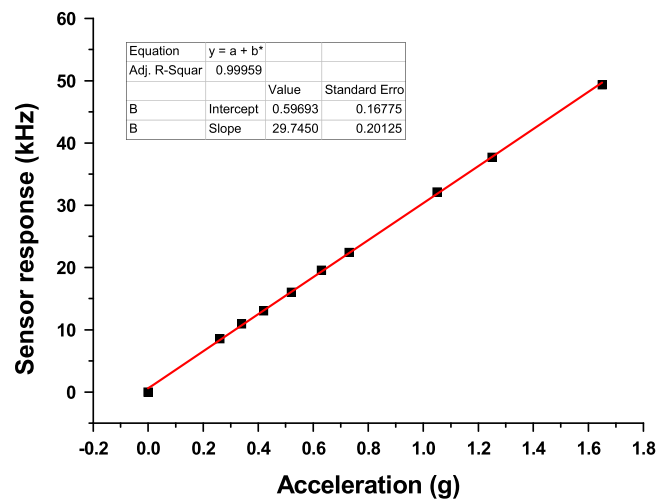


Figure 10. The sensitivity evaluation of the SAW acceleration sensor.

accelerometer. To avoid the thread from the larger impact force from the vibration table, the test acceleration range is limited to ~2 g. Figure 9 shows the continuous response of the stimulated sensor at various accelerations. The frequency

Table 2. Design parameters of the acceleration sensor.

Design parameters	Values	Design parameters	Values
IDT length (λ)	41	Al electrode thickness (nm)	150
Reflector length (λ)	150	Beam length (mm)	20
Distance between IDTs (λ)	10.25	Beam width (mm)	1.5
Distance between IDT and reflector (λ)	0.25	Beam thickness (mm)	0.2
Aperture (λ)	80	Proof mass and beam mass ratio	5

response to the acceleration was recorded every 18 ms so that one point on the graph corresponds to an 18 ms interval. The transit response is from the transitory shocks of the vibration table. It consists of the sum of the transient responses. The magnitude of the recording signals is proportional to the acceleration, as shown in figure 10. The measured results indicate a high sensitivity of $\sim 29.7 \text{ kHz g}^{-1}$, and good linearity was obtained. Also, it is much higher than the reported values from the similar sensor structure [2]. In addition, good agreement was observed among the measured acceleration sensitivity and calculated result.

Usually, the detection limit in acceleration closely relates to the frequency stability of the oscillator. Considering the measured short-term stability of 1 Hz s^{-1} and the 29.7 kHz in response to the acceleration of 1 g , the threshold detection limit of the developed accelerometer was expected to be $\sim 1 \times 10^{-4} \text{ g}$. The measured results indicate that the developed SAW accelerometer is very promising for inertial applications.

5. Conclusion

A SAW-based accelerometer incorporated with a ST-X quartz cantilever beam was successfully demonstrated. The response mechanism was analyzed theoretically, and the optimal dimension of the cantilever beam was determined. The differential frequency signal of the resonator-oscillator configuration was utilized for acceleration characterization. Using the precision vibration table, the developed SAW-based accelerometer was evaluated, and the obtained sensitivity and threshold detection limit were 30 kHz g^{-1} and $\sim 1 \times 10^{-4} \text{ g}$, respectively.

Acknowledgments

The author gratefully acknowledges the support of the ‘The Hundred Talents Program’ of Chinese Academy of Sciences,

and the National Natural Science Foundation of China: no. 11374254.

References

- [1] Jiang H, Lu W W and Li Y Y 2012 Analysis of a novel SAW acceleration sensor with cantilever beam using ST-X quartz *Appl Mech. Mater.* **189** 285–9
- [2] Williams J T 2003 Surface acoustic wave (SAW) accelerometer *United States Patent US* 6553836
- [3] Hartemann P and Meunier P L 1981 Surface acoustic wave accelerometer *Proc. IEEE Ultrasonics Symp.* pp 52–4
- [4] Bower D and Creacknell M 1987 A high linearity SAW accelerometer *41st Annual Frequency Control* pp 544–7
- [5] Natale C D, Davide F, Amico A D and Saggio G 1994 Multicomponent analysis of a Tri-axial accelerometer based on surface acoustic wave sensors *Proc. IEEE Ultrasonics Symp.* pp 495–8
- [6] Jaime O G and Pablo R P 2011 Relationship between acceleration and the scattering matrix in a SAW-MEMS accelerometer *IEEE Trans. UFFC* **58** 1460–7
- [7] Filipiak J, Solarz L and Zubko K 2004 The analysis of acceleration sensor by the discrete model *Mol. Quantum Acoust.* **25** 89–99
- [8] Filipiak J, Kopycki C, Solarz L and Ostrowski J 1997 Lithium niobate as the substrate for the SAW acceleration sensor *Proc. SPIE* **3179** 256
- [9] Filipiak J and Kopycki C 1999 Surface acoustic waves for the detection of small vibration *Sensors Actuators* **76** 318–22
- [10] Filipiak J, Solarz L and Steczko G 2011 Surface acoustic wave (SAW) vibration sensors *Sensors* **11** 11809–31
- [11] Zhang X, Wang F and Li L 2007 Optimal selection of piezoelectric substrates and crystal cuts for SAW-based pressure and temperature sensors *IEEE Trans. UFFC* **54** 1207–16
- [12] Wang S, Dong Y and Feng G 1999 Research on characteristics of resonant SAW accelerometer *Piezoelectrics & Acoustooptics* **21** 164–7
- [13] Wang W, Xie X and He S 2013 Optimal design of a polyaniline-coated surface acoustic wave based humidity sensor *Sensors* **13** 16816–28
- [14] Wang W, Oh H, Lee K, Yoon S and Yang S 2009 Enhanced sensitivity of novel surface acoustic wave microelectromechanical system-interdigital transducer gyroscope *Jpn. J. Appl. Phys.* **48** 06FK09